

$\bar{K}N$ INTERACTION AND KAONS IN THE NUCLEAR MEDIUM

A. RAMOS

*Departament d'Estructura i Constituents de la Matèria, Universitat de Barcelona,
Diagonal 647, 08028 Barcelona, Spain*

E. OSET

*Departamento de Física Teórica and IFIC, Universidad de Valencia-CSIC,
46100 Burjassot (Valencia), Spain*

The s-wave meson-nucleon interaction in the $S = -1$ sector is studied by means of a coupled-channel Lippmann Schwinger equation, using the lowest order chiral Lagrangian and a cut off to regularize the loop integrals. The position and width of the $\Lambda(1405)$ resonance and the K^-p scattering cross sections at low energies are well reproduced. The inclusion of the $\eta\Lambda, \eta\Sigma^0$ channels in the coupled system is found very important and allows a solution in terms of only the lowest order Lagrangian. The model is applied to calculate the in-medium K^- self-energy to which we add a small p-wave piece resulting from the coupling to hyperon particle-nucleon hole excitations. The K^- feels an attraction of about -100 MeV at normal nuclear density. The $\Lambda(1405)$ resonance shifts to energies above the K^-p threshold and ends up dissolving as density increases. It remains to be seen how these effects persist when the dressing of the \bar{K} and the π mesons is incorporated self-consistently in the calculation.

1 Introduction

Understanding the interaction of kaons (K^+, K^0) and antikaons (\bar{K}^0, K^-) with hadrons is of especial interest for different branches of nuclear physics. From the more fundamental point of view, the fact that these mesons contain a strange quark, with a mass not so small compared with the scale of chiral symmetry breaking, poses a severe test on the chiral Lagrangians. Moreover, due to the different quark/antiquark content, the $K^+ = (u\bar{s})$ and the $K^- = (\bar{u}s)$ interact very differently with nucleons. The K^-p interaction, for instance, is dominated by the presence of a resonance, the $\Lambda(1405)$, which in a quark picture appears very naturally from the annihilation of the \bar{u} quark. Investigating whether the chiral Lagrangians, written in terms of mesonic and baryonic degrees of freedom, can account for the differences between the KN and $\bar{K}N$ interactions is also a very challenging task.

The properties of the kaons and antikaons in the nuclear medium have been the object of numerous investigations since the possibility of the existence of a kaon condensed phase in dense nuclear matter was pointed out¹. The presence of strangeness would influence the behaviour of dense matter due to the soften-

ing of the nuclear equation of state. Most of the recent works start from chiral Lagrangians that reproduce the free space scattering properties. The $\Lambda(1405)$ resonance is either introduced as an elementary field² or dynamically generated through a Lippmann-Schwinger equation^{3,4,5}. Pauli blocking acting on the intermediate nucleon states makes the $\bar{K}N$ interaction density dependent which, in turn, modifies the K^- properties in the medium. Medium effects at the simpler mean field level have been also studied in the context of chiral Lagrangians⁶ or with relativistic Walecka-type models extended to incorporate strangeness in the form of hyperons or kaons⁷.

All the different approaches agree qualitatively in establishing that, in the medium, the K^+ feels a moderate repulsion and the K^- a strong attraction. How large is this attraction is still a subject under intense debate. Phenomenological approaches⁸ based on fits to kaonic atom data find a K^- -nucleus potential of the order of -200 ± 20 MeV in the nuclear center. However, no calculation that starts from the bare K^-N interaction predicts such an attraction, the values ranging from -120 to -100 MeV. Hopefully, heavy-ion reactions, that are sensitive to higher density regions, will help in elucidating these discrepancies. At the same time, it is necessary to develop theories that treat the intricacies associated to the mutual interaction between all the hadrons in the medium as accurately as possible.

2 $\bar{K}N$ interaction in free space

The effective chiral Lagrangian formalism, which has been very successful in explaining the properties of meson-meson interaction at low energies^{9,10}, has also proved to be an excellent tool to study the meson-baryon system^{11,12} when the interaction is weak, as in the case of the s-wave πN and K^+N interaction. However, in the $S = -1$ sector, the $\bar{K}N$ system couples strongly to many other channels and generates a resonance below threshold, the $\Lambda(1405)$. In this case the standard chiral scheme, an expansion in powers of the typical momenta involved in the process, fails to be an appropriate approach.

A non perturbative scheme, consisting of solving a set of coupled-channel Lippmann Schwinger equations using the lowest and next to lowest order chiral Lagrangians, was employed in Ref.¹³. The channels included were $\bar{K}N$, $\pi\Lambda$ and $\pi\Sigma$ which are those opened at the K^-p threshold. Although a good description of the $\Lambda(1405)$ resonance and the low energy K^-p cross sections was obtained with only the lowest order Lagrangian, the well measured threshold branching ratio, $\gamma = \frac{\Gamma(K^-p \rightarrow \pi^+\Sigma^-)}{\Gamma(K^-p \rightarrow \pi^-\Sigma^+)}$, was poorly reproduced. This motivated the authors to include the $O(q^2)$ terms of the chiral Lagrangian in the fit, at the expense of introducing new parameters.

The success of this unitary coupled channel method stimulated work in the meson-meson sector¹⁴ and an excellent reproduction of the resonances in the scalar sector, plus phase shifts and inelasticities in the different physical channels was obtained, by means of coupled-channel Lippmann Schwinger equations using the lowest order chiral Lagrangian, plus a suitable cut off.

The model presented here extends the ideas of¹⁴ to the $\bar{K}N$ sector. Although our approach shares many similarities with that of Ref.¹³, the main difference lies in that our coupled equations also include the channels $\eta\Lambda$, $\eta\Sigma$ and $K\Xi$, which lie, respectively, 230 MeV, 310 MeV and 380 MeV above the K^-p threshold. As we will see, the inclusion of these channels, especially the $\eta\Lambda$, allows to describe all the low energy scattering data, including the ratio γ , with only the lowest order Lagrangian.

2.1 Meson-baryon amplitudes from the chiral Lagrangian

The lowest order chiral Lagrangian, coupling the octet of pseudoscalar mesons to the octet of $1/2^+$ baryons, is

$$L_1^{(B)} = \langle \bar{B}i\gamma^\mu \nabla_\mu B \rangle - M_B \langle \bar{B}B \rangle + \frac{1}{2}D \langle \bar{B}\gamma^\mu \gamma_5 \{u_\mu, B\} \rangle + \frac{1}{2}F \langle \bar{B}\gamma^\mu \gamma_5 [u_\mu, B] \rangle, \quad (1)$$

where the symbol $\langle \rangle$ denotes trace of SU(3) matrices and

$$\begin{aligned} \nabla_\mu B &= \partial_\mu B + [\Gamma_\mu, B] \\ \Gamma_\mu &= \frac{1}{2}(u^\dagger \partial_\mu u + u \partial_\mu u^\dagger) \\ U &= u^2 = \exp(i\sqrt{2}\Phi/f) \\ u_\mu &= iu^\dagger \partial_\mu U u^\dagger. \end{aligned} \quad (2)$$

The SU(3) matrices for the mesons and the baryons are the following

$$\Phi = \begin{pmatrix} \frac{1}{\sqrt{2}}\pi^0 + \frac{1}{\sqrt{6}}\eta & \pi^+ & K^+ \\ \pi^- & -\frac{1}{\sqrt{2}}\pi^0 + \frac{1}{\sqrt{6}}\eta & K^0 \\ K^- & \bar{K}^0 & -\frac{2}{\sqrt{6}}\eta \end{pmatrix}, \quad (3)$$

$$B = \begin{pmatrix} \frac{1}{\sqrt{2}}\Sigma^0 + \frac{1}{\sqrt{6}}\Lambda & \Sigma^+ & p \\ \Sigma^- & -\frac{1}{\sqrt{2}}\Sigma^0 + \frac{1}{\sqrt{6}}\Lambda & n \\ \Xi^- & \Xi^0 & -\frac{2}{\sqrt{6}}\Lambda \end{pmatrix}. \quad (4)$$

At lowest order in momentum the interaction Lagrangian reduces to

$$L_1^{(B)} = \langle \bar{B}i\gamma^\mu \frac{1}{4f^2} [(\Phi \partial_\mu \Phi - \partial_\mu \Phi \Phi)B - B(\Phi \partial_\mu \Phi - \partial_\mu \Phi \Phi)] \rangle. \quad (5)$$

The coupled channel formalism requires to evaluate the transition amplitudes between the 10 different channels that can be built from the meson and baryon octets, namely K^-p , \bar{K}^0n , $\pi^0\Lambda$, $\pi^0\Sigma^0$, $\pi^+\Sigma^-$, $\pi^-\Sigma^+$, $\eta\Lambda$, $\eta\Sigma^0$, $K^+\Xi^-$ and $K^0\Xi^0$. These amplitudes have the form

$$V_{ij} = -C_{ij} \frac{1}{4f^2} \bar{u}(p_i) \gamma^\mu u(p_j) (k_{i\mu} + k_{j\mu}) , \quad (6)$$

where $p_j, p_i(k_j, k_i)$ are the initial, final momenta of the baryons (mesons). The explicit values of the coefficients C_{ij} can be found in ref. ¹⁵. At low energies we can neglect the spatial components and Eq. (6) simplifies to

$$V_{ij} = -C_{ij} \frac{1}{4f^2} (k_j^0 + k_i^0) . \quad (7)$$

2.2 Coupled-channel Lippmann Schwinger equations

The coupled-channel Lippmann Schwinger equations in the center of mass frame read:

$$T_{ij} = V_{ij} + \overline{V_{il} G_l T_{lj}} \quad (8)$$

where the indices i, l, j run over all possible channels and

$$\overline{V_{il} G_l T_{lj}} = i \int \frac{d^4q}{(2\pi)^4} \frac{M_l}{E_l(\vec{q})} \frac{V_{il}(k_i, q) T_{lj}(q, k_j)}{k^0 + p^0 - q^0 - E_l(\vec{q}) + i\epsilon} \frac{1}{q^2 - m_l^2 + i\epsilon} , \quad (9)$$

with M_l, E_l and m_l being the baryon mass, baryon energy and meson mass in the intermediate state. The integral is regularized through a cut off, q_{\max} , which is the free parameter of our model.

Although Eq. (9) requires the half-off-shell amplitudes, we can show, similarly as in Ref. ¹⁴, that the off-shell part of the amplitude goes into renormalization of coupling constants. We take, as an example, the second order (one-loop) term in the Lippmann Schwinger series with equal masses in the external and intermediate states for simplicity. We have

$$\begin{aligned} V_{\text{off}}^2 &= C(k^0 + q^0)^2 = C(2k^0 + q^0 - k^0)^2 \\ &= C^2(2k^0)^2 + 2C(2k^0)(q^0 - k^0) + C^2(q^0 - k^0)^2 , \end{aligned} \quad (10)$$

with C a constant. The first term in the last expression is the on shell contribution V_{on}^2 ($V_{\text{on}} \equiv C2k^0$). Neglecting $p^0 - E(\vec{q})$ in Eq. (9), typical approximation in the heavy baryon formalism, the $(q^0 - k^0)$ factor of the second term in Eq. (10) cancels the baryon propagator. The contribution is proportional to V_{on} and, therefore, is already absorbed by the first order (no loop) term because the

physical coupling f is used. Similarly, the term proportional to $(q^0 - k^0)^2$ will cancel the $(k^0 - q^0)$ term in the denominator. The remaining factor, $(k^0 - q^0)$, contains a term proportional to k^0 (and hence V_{on}) and a term proportional to q^0 which vanishes for parity reasons. Similar arguments can be used in the case of coupled channels and higher order loops and the conclusion is that we can factorize V_{on} and T_{on} outside the integral of Eq. (9). As a consequence, the integral equation reduces to a set of algebraic equations and the loop integral reads

$$\begin{aligned}
G_l &= i \int \frac{d^4 q}{(2\pi)^4} \frac{M_l}{E_l(\vec{q})} \frac{1}{k^0 + p^0 - q^0 - E_l(\vec{q}) + i\epsilon} \frac{1}{q^2 - m_l^2 + i\epsilon} \\
&= \int_{|\vec{q}| < q_{\text{max}}} \frac{d^3 q}{(2\pi)^3} \frac{1}{2\omega_l(\vec{q})} \frac{M_l}{E_l(\vec{q})} \frac{1}{\sqrt{s} - \omega_l(\vec{q}) - E_l(\vec{q}) + i\epsilon} \quad (11)
\end{aligned}$$

with $\sqrt{s} = p^0 + k^0$.

Our model depends on a free parameter, q_{max} , which is determined such that, for a fixed value of f chosen between $f_\pi = 93$ MeV and $f_K = 1.22f_\pi$, we get the best reproduction of the threshold ratios: γ , $R_c = \frac{\Gamma(K^- p \rightarrow \text{charged particles})}{\Gamma(K^- p \rightarrow \text{all})}$ and $R_n = \frac{\Gamma(K^- p \rightarrow \pi^0 \Lambda)}{\Gamma(K^- p \rightarrow \text{all neutral states})}$. The precise value of f is the one that gives the best agreement with the $\Lambda(1405)$ properties seen in the $\pi\Sigma$ mass spectrum. Our optimal choice was found for $f = 1.15f_\pi$ and $q_{\text{max}} = 630$ MeV.

2.3 $K^- p$ scattering observables

The results for the threshold ratios are shown in Table 1 where they are compared with those obtained omitting the η channels. We can see that the three ratios are reproduced within 5%. The ratio γ is reduced by a factor 2.2 when the η channels are omitted. This small value for γ is compatible with that obtained in¹³, which motivated the authors of that work to incorporate higher order terms in the chiral expansion and perform a global fit with five parameters.

Table 1: Threshold ratios

	γ	R_c	R_n
All channels	2.32	0.627	0.213
No η	1.04	0.637	0.158
exp. ^{16,17}	2.36 ± 0.04	0.664 ± 0.011	0.189 ± 0.015

The K^-p cross sections in all channels, given by

$$\sigma_{ij} = \frac{1}{4\pi} \frac{M_i M_j}{s} \frac{k_i}{k_j} |T_{ij}|^2 \quad (12)$$

with $j = 1$ (K^-p), are then calculated with the best choice of parameters and have not been used in a best fit to the data. Our results for some selected channels ($K^-p \rightarrow K^-p, \bar{K}^0n, \pi^+\Sigma^-, \pi^-\Sigma^+$) are compared with the low-energy scattering data in Fig. 1. We show the cross sections obtained with the full basis of physical states (solid line), with the isospin basis which uses average masses for \bar{K}, π, N and Σ (short-dashed line), and omitting the coupling to the intermediate η channels (long-dashed line). The results using the isospin basis are close to those using the basis of physical states but the cusp associated to the opening of the \bar{K}^0n channel appears in the wrong place. The effects of the η channels are much more spectacular. Close to threshold, the $\pi^-\Sigma^+$ cross section is reduced by almost a factor of 3 and the $\pi^+\Sigma^-$ cross section is reduced by a factor 1.3 when the η channels are included. This enhances the ratio γ by a factor 2.2 and makes the agreement with the experimental value possible using only the lowest order chiral Lagrangian.

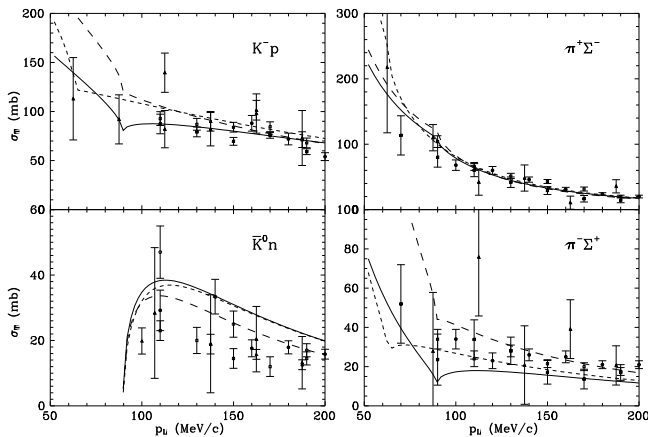


Figure 1: K^-p scattering cross sections as functions of the K^- momentum in the lab frame: with the full basis of physical states (solid line), omitting the η channels (long-dashed line) and with the isospin-basis (short-dashed line).

Finally, the K^-p and K^-n scattering lengths, defined as

$$a_i = -\frac{1}{4\pi} \frac{M}{\sqrt{s}} T_{ii} \quad i = K^-p \text{ or } K^-n, \quad (13)$$

are presented in Table 2. We observe that isospin breaking effects in the K^-n amplitude, as well as those omitting the η channel, are moderate in this case. We should note that this is an isospin $I = 1$ channel where the K^-p scattering length is essentially in agreement with the most recent results from Kaonic hydrogen X rays¹⁸. Our results are also in qualitative agreement with the scattering lengths determined from scattering data in¹⁹ which have an estimated error of 15%. Note that these results are obtained from the isospin scattering lengths but as we can see from our calculations shown in Table 2 there are violations of isospin at the level of 20% in these amplitudes. It is also worth calling the attention to the remarkable agreement of our results for the real part of the scattering lengths with those obtained in¹⁹ from a combined dispersion relation and M matrix analysis.

Table 2: K^-N scattering lengths

	a_{K^-p} (fm)	a_{K^-n} (fm)
Full basis	$-1.00 + i0.94$	$0.53 + i0.62$
No η	$-0.68 + i1.64$	$0.47 + i0.53$
Isos. basis	$-0.85 + i1.24$	$0.54 + i0.54$
Exp. ¹⁸	$(-0.78 \pm 0.18) + i(0.49 \pm 0.37)$	
Exp. ¹⁹	$-0.67 + i0.64$	$0.37 + i0.60$
Exp. $Re(a)$ ¹⁹	-0.98	0.54

3 \bar{K} in the nuclear medium

The dynamics of the $\bar{K}N$ interaction at low energies is dominated by the $\Lambda(1405)$ resonance, an isospin $I = 0$ quasi-bound K^-p state. As a result, the isospin averaged $\bar{K}N$ interaction is repulsive in free space. However, kaonic atom data suggest that the K^- feels a strongly attractive potential at nuclear densities $\rho \sim \rho_0$, where ρ_0 is normal nuclear matter density. This implies a rapid transition from a repulsive $\bar{K}N$ interaction to an attractive one as density increases and, therefore, the study of the K^- properties in the medium cannot be done in terms of the simple $T\rho$ or impulse approximation. It is therefore necessary to consider the density dependence of the in-medium $\bar{K}N$ interaction, $T^{\text{eff}}(\rho)$.

3.1 Pauli blocking

One source of density dependence comes from the Pauli principle, which prevents the scattering to intermediate nucleon states below the Fermi momentum, p_F , and ends up blocking the appearance of the $\Lambda(1405)$ resonance. In Fig. 2 we show the real (solid lines) and imaginary (dashed lines) parts of the in-medium scattering length as functions of \sqrt{s} for the scattering of a K^- with a proton at rest. The results are shown for $p_F = 0, 150$ and 300 MeV/c and, as density increases, the $\Lambda(1405)$ resonance moves to higher values of \sqrt{s} , hence changing from being slightly below the K^-p threshold (denoted by the vertical line) at $p_F = 0$ MeV/c to being above it from a certain density on. It is also clearly seen that, already at $p_F = 150$ MeV/c, the scattering length at threshold is positive, which means that the in-medium K^-p interaction has become attractive.

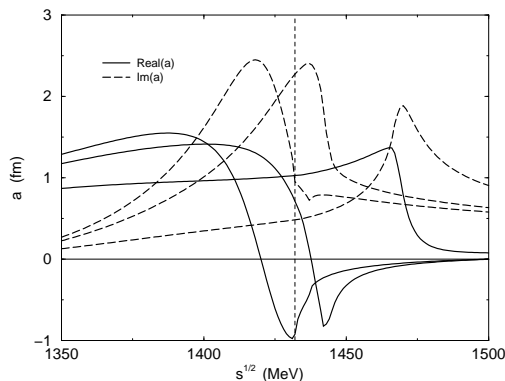


Figure 2: Real (solid line) and Imaginary (dashed line) parts of the K^-p scattering length at three different Fermi momenta $p_F = 0, 150$ and 300 MeV/c.

The K^- properties in the medium can be derived from the K^- self-energy (or optical potential) which is obtained by summing up the in-medium $\bar{K}N$ interaction for all the nucleons filling up the Fermi sea:

$$\Pi_K^s(q^0, \vec{q}, \rho) = 2 \int \frac{d^3p}{(2\pi)^3} \theta(p_F - |\vec{p}|) \left[T_{K^-p}^{\text{eff}}(\sqrt{s}, \rho) + T_{K^-n}^{\text{eff}}(\sqrt{s}, \rho) \right]. \quad (14)$$

We find that the averaged in-medium interaction defined as $\bar{T}^{\text{eff}}(\sqrt{s}, \rho) = \Pi_K^s(q^0 = m_K, \vec{q} = 0, \rho)/\rho$ becomes attractive around $\rho \simeq 0.17\rho_0$ ($p_F \simeq 150$

MeV/c). The solution of the new K^- dispersion relation

$$\omega^2 = \vec{q}^2 + m_K^2 + \Pi_K^s(\omega, \vec{q}, \rho) , \quad (15)$$

determines the effective mass, $m_K^* = \text{Re}\omega(\vec{q} = 0)$, and decay width, $\Gamma = -2\text{Im}\omega(\vec{q} = 0)$, of the K^- meson in the medium. In Fig. 3 we show the K^- effective mass in units of the bare mass as a function of the density for neutron matter (dashed line) and symmetric nuclear matter (solid line). The effective mass shows a strong non-linear density dependence at very small densities in symmetric nuclear matter due to the influence of the $\Lambda(1405)$ resonance in the K^-p interaction. As density increases, the K^- pole lies far away from its free space value and the effect of the resonance, if still present, is negligible. At ρ_0 we find $m_K^* = 403$ MeV, implying an equivalent s-wave K^- -nucleus potential $U_{K^-} = \Pi_K^s/2\omega \simeq -100$ MeV, much smaller in magnitude than the value suggested by the atomic data analyses. The decay width of the K^- is relatively small and amounts to $\Gamma = 34$ MeV. Our results for the in-medium $\bar{K}N$ interaction and the K^- properties are in qualitative agreement with those of Ref. ⁴, where the chiral approach of ¹³ with the updated parameters of ²⁰ is used.

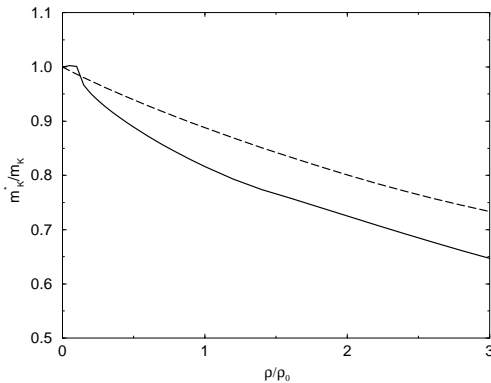


Figure 3: Effective mass of the K^- as a function of density in neutron matter (dashed line) and symmetric nuclear matter (solid line).

3.2 Many-body correlations

If Pauli blocking can affect so drastically the behaviour of the K^- in the medium with respect to that in free space it is reasonable to investigate other sources of density dependence which are, a priori, equally important. In particular, all the mesons and baryons participating in the intermediate loops interact with the nucleons of the Fermi sea and, as a consequence, feel an optical potential which changes the threshold energy of the different channels.

For the time being, we are going to assume that all the relevant baryons (N, Λ, Σ) feel the same moderately attractive potential, which cancels out in the differences involved in the energy balances. We will instead focus our attention on the dressing of the mesons, particularly that of \bar{K} and π since the η appears in intermediate states that lie quite far above the K^-p threshold.

The model discussed here provides a s-wave K^- self-energy [Eq. (14)] to which we also add a p-wave contribution coming from the coupling of the \bar{K} meson to hyperon particle–nucleon hole excitations:

$$\Pi_K^p(q, \rho) = \frac{1}{2} \left(\frac{g_{N\Lambda K}}{2M} \right)^2 \vec{q}^2 U_\Lambda(q, \rho) + \frac{3}{2} \left(\frac{g_{N\Sigma K}}{2M} \right)^2 \vec{q}^2 U_\Sigma(q, \rho) , \quad (16)$$

where $g_{N\Lambda K}, g_{N\Sigma K}$ are the SU(3) strong coupling constants and $U_Y(q, \rho)$ is the Lindhard function for a hyperon particle-nucleon hole excitation. This p-wave contribution can become important for large values of the K^- momentum.

For the pion self-energy we take that of Ref. ²¹ which consists of a small constant s-wave part, $\Pi_\pi^s(\rho)$, plus a p-wave part, $\Pi_\pi^p(q, \rho)$, modified by the effect of short range nuclear correlations through the typical g' Landau parameter (slightly momentum dependent):

$$\Pi_\pi^p(q, \rho) = \left(\frac{f}{m_\pi} \right)^2 \vec{q}^2 \frac{U_\pi(q, \rho)}{1 - \left(\frac{f}{m_\pi} \right)^2 g'(q) U_\pi(q, \rho)} , \quad (17)$$

where $U_\pi(q, \rho) = U_N(q, \rho) + U_\Delta(q, \rho) + U_{2p2h}(q, \rho)$ contains the Lindhard functions for particle-hole and Δ -hole excitations plus a piece coming from the coupling to 2 particle-2 hole excitations.

The dressed meson propagator reads ($i = \bar{K}, \pi$):

$$D_i(q, \rho) = \frac{1}{(q^0)^2 - \vec{q}^2 - m_i^2 - \Pi_i(q, \rho)} = \int_0^\infty d\omega 2\omega \frac{S_i(\omega, \vec{q}, \rho)}{(q^0)^2 - \omega^2 + i\epsilon} , \quad (18)$$

written in terms of the self-energy (second term) or the spectral density (last term) which is defined as $S_i(\omega, \vec{q}, \rho) = -\text{Im } D_i(\omega, \vec{q}, \rho)/\pi$.

The real (solid lines) and imaginary (dashed lines) parts of the s- and p-wave K^- self-energy at ρ_0 are shown in Fig. 4 as functions of q_0 for a K^- momentum $q=200$ MeV/c. The p-wave self-energy shows the typical shape of two Lindhard functions, corresponding to the Λ^- and Σ^- -hole excitations, and is located at low q_0 values, where the contribution of the real part is comparable to that of the s-wave self-energy. However, the position of the new K^- pole is basically determined by the dominant s-wave piece, especially for low momentum values. This can be seen in Fig. 5, where the K^- spectral density is plotted as a function of q_0 for a momentum $q=100$ MeV/c and for several densities. The p-wave self-energy is responsible for the appearance of some extra strength, barely seen on the scale of the figure, to the left of the peaks. At $\rho_0 = \rho_0/4$ a two-mode excitation is clearly visible. The left peak corresponds to the K^- pole branch, appearing at an energy smaller than m_K due to the attractive medium effects, and the right one corresponds to the $\Lambda(1405)$ -hole state, which is located above m_K due to Pauli blocking which shifts the $\Lambda(1405)$ resonance to higher energies. This last excitation mode disappears as density increases, reflecting the fact that the $\Lambda(1405)$ dissolves in dense matter.

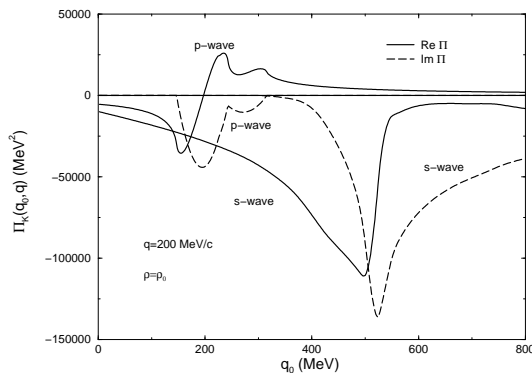


Figure 4: Kaon self-energy.

The pion spectral density at ρ_0 is shown in Fig. 6 as a function of q_0 for several momentum values. Each peak shows the position of the corresponding medium modified pion pole and the structures at the left show the strength due to particle-hole excitations. It is clearly seen that the deviation from the

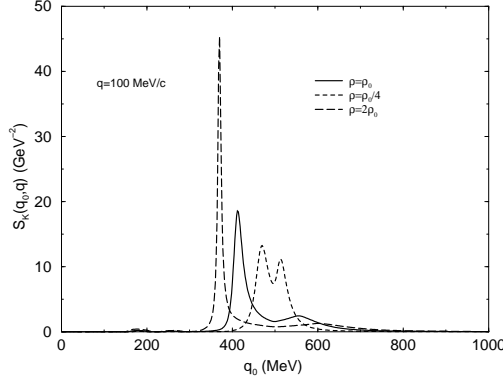


Figure 5: K^- spectral density for a momentum $q = 100 \text{ MeV}/c$ at several densities: $\rho_0/4$ (short-dashed line), ρ_0 (solid line) and $2\rho_0$ (long-dashed line).

free pion energy, $\sqrt{m_\pi^2 + \vec{q}^2}$, increases as the momentum increases and this moves the $\pi\Sigma$ and $\pi\Lambda$ thresholds of the intermediate states in the loops to much lower energies.

The influence of the dressed mesons can be included in the scheme by replacing the free meson propagator in Eq. (11) by that of Eq. (18). Then, taking the Pauli principle on the nucleons also into account, the loop integral becomes

$$G_l(\sqrt{s}, \vec{P}, \rho) = \int_0^\infty d\omega \int_{|\vec{q}| < q_{max}} \frac{d^3q}{(2\pi)^3} \frac{M_l}{E_l(\vec{q})} S_l(\omega, \vec{q}, \rho) \times \left\{ \frac{\theta(|\vec{P} - \vec{q}| - p_F)}{\sqrt{s} - \omega - E_l(\vec{q}) + i\epsilon} + \frac{\theta(p_F - |\vec{P} - \vec{q}|)}{\sqrt{s} - \omega - E_l(\vec{q}) - i\epsilon} \right\}. \quad (19)$$

When the dressing of the K^- is incorporated, the problem needs to be solved self-consistently since the loop integral of Eq. (19), required to obtain the in-medium $\bar{K}N$ interaction, T^{eff} , and thus the K^- self-energy through Eq. (14), also depends on the K^- propagator. A self-consistent calculation has been attempted in Ref. ⁵, where it is found that the repulsive shift on the $\Lambda(1405)$ mass induced by Pauli blocking is compensated by the use of an attractive K^- self-energy in the intermediate states. The mass of the resonance turns out to be close to its free space value and the width becomes larger as density increases.

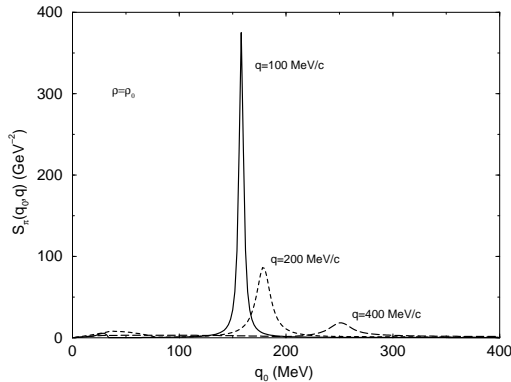


Figure 6: Pion spectral density at ρ_0 for several momentum values: 100 (solid line), 200 (short-dashed line) and 400 (long-dashed line) MeV/c.

Work is in progress to check these predictions within our model, which also attempts at incorporating the strong medium modifications of the pion.

4 Conclusions

We have studied the s-wave $\bar{K}N$ interaction on the basis of a coupled-channel Lippmann Schwinger equation, using the lowest order chiral Lagrangian and one cut-off parameter. This simple model gives an excellent agreement with all the low energy scattering data and the role of the η intermediate channels, omitted in previous investigations, has been found crucial.

We apply this model to the study of the K^- properties in the nuclear medium. Pauli blocking on the intermediate nucleon states produces a positive shift on the mass of the $\Lambda(1405)$, which ends dissolving in the medium at densities close to normal nuclear matter density. The K^- optical potential is around -100 MeV, half of what is obtained from K^- atom data analyses.

Both the K^- self-energy, to which we also add a small p-wave from hyperon particle-nucleon hole excitations, and the strongly attractive pion self-energy need to be incorporated self-consistently in the loops before any conclusion on the in-medium $\Lambda(1405)$ properties can be drawn.

Acknowledgments

This work is partially supported by DGICYT contract numbers PB95-1249 and PB96-0753, and by the EEC-TMR Program under contract No. CT98-0169.

References

1. D.B. Kaplan and A.E. Nelson, *Phys. Lett.* **B175**, 57 (1986)
2. C.H. Lee, G.E. Brown, D.P. Min and M. Rho, *Nucl. Phys.* **A385**, 481 (1995); C.H. Lee, *Phys. Rep.* **275**, 255 (1996)
3. V. Koch, *Phys. Lett.* **B337**, 7 (1994)
4. T. Waas, N. Kaiser and W. Weise, *Phys. Lett.* **B365**, 12 (1996); **B379**, 34 (1996); T. Waas and W. Weise, *Nucl. Phys.* **A625**, 287 (1997)
5. M. Lutz, *Phys. Lett.* **B426**, 12 (1998)
6. G.Q. Li, C.H. Lee and G.E. Brown, *Nucl. Phys.* **A625**, 372 (1997)
7. J. Schaffner and I.N. Mishustin, *Phys. Rev.* **C53**, 1416 (1996); J. Schaffner-Bielich, I.N. Mishustin and J. Bondorf, *Nucl. Phys.* **A625**, 325 (1997)
8. E. Friedman, A. Gal, C.J. Batty, *Nucl. Phys.* **A579**, 518 (1994)
9. J. Gasser and H. Leutwyler, *Nucl. Phys.* **B250**, 465 (1985)
10. A. Pich, *Rep. Prog. Phys.* **58**, 563 (1995)
11. G. Ecker, *Prog. Part. Nucl. Phys.* **35**, 1 (1995)
12. V. Bernard, N. Kaiser and U.G. Meissner, *Int. J. Mod. Phys.* **E4**, 193 (1995)
13. N. Kaiser, P.B. Siegel and W. Weise, *Nucl. Phys.* **A594**, 325 (1995)
14. J.A. Oller and E. Oset, *Nucl. Phys.* **A620**, 438 (1997)
15. E. Oset and A. Ramos, *Nucl. Phys.* **A635**, 99 (1998)
16. R.J. Nowak et al., *Nucl. Phys.* **B139**, 61 (1978)
17. D.N. Tovee et al., *Nucl. Phys.* **B33**, 493 (1971)
18. M. Iwasaki et al., *Phys. Rev. Lett.* **78**, 3067 (1997)
19. A.D. Martin, *Nucl. Phys.* **B179**, 33 (1981)
20. N. Kaiser, T. Waas and W. Weise, *Nucl. Phys.* **A612**, 297 (1997)
21. A. Ramos, E. Oset and L.L. Salcedo, *Phys. Rev.* **C50**, 2314 (1994)